



EC-STM Studies of Te and CdTe Atomic Layer Formation from a Basic Te Solution

Marcus D. Lay and John L. Stickney*^z

Department of Chemistry, University of Georgia, Athens, Georgia 30602, USA

The cyclic voltammetry of Te on Au is markedly affected by pH. This fact can be used to advantage when designing an electrodeposition cycle for CdTe. For instance, if a pH 2 Te solution is used, the underpotential deposition (UPD) potential for Te is 0.8 V positive of that for Cd. However, if a pH 9.2 Te deposition solution is used, the potential for Te UPD coincides with that for Cd, greatly simplifying the development of an electrochemical atomic layer epitaxy (EC-ALE) cycle. This report describes electrochemical scanning tunneling microscopy (EC-STM) studies of Te deposition on Au(111) and Au(100) from basic media. Several structures were observed on Au(111): a (6×6) tellurite adlayer which spontaneously adsorbed prior to Te formation, a $1/4$ coverage (2×2) -Te, and a $1/3$ coverage $(2 \times \sqrt{10})$ -Te. While on Au(111), a $1/3$ coverage $(\sqrt{3} \times \sqrt{3})$ -Te with (13×13) light domain walls, and two (3×3) -Te structures, with coverages of $4/9$ and $5/9$, were observed. Results of the formation of the first CdTe compound monolayer using an EC-ALE cycle which includes Te deposition from a basic solution are also included.

© 2004 The Electrochemical Society. [DOI: 10.1149/1.1723497] All rights reserved.

Manuscript submitted July 10, 2003; revised manuscript received December 1, 2003. Available electronically May 5, 2004.

Chalcogenides and their reactivity are immensely important, as exemplified by the role of oxygen in the oxidation of metals. The rest of the chalcogenides are important as well, with roles in oxidation,¹⁻³ self-assembled monolayer formation,^{4,5} surface passivation, and the formation of II-VI and IV-VI compound semiconductors.^{6,7} Te in particular, as a constituent of CdTe, is an important optoelectronic material.^{8,9} Compound semiconductors are typically electrodeposited from a single bath, containing precursors for all the constituent elements, in a process referred to as codeposition. More recently, a number of Te-containing compounds, such as CdTe, have been electrodeposited using a method referred to as electrochemical atomic layer epitaxy (EC-ALE).¹⁰ EC-ALE is the electrochemical analogue of atomic layer epitaxy (ALE). ALE is based on the use of surface-limited reactions to grow compounds one atomic layer at a time. Historically, ALE reactions have been controlled using the temperature of the substrate and/or reactants.

In electrochemistry, surface-limited reactions are generally controlled by the potential and referred to as underpotential deposition (UPD). UPD refers to the phenomenon by which an element electrodeposits on another at a potential prior to its Nernstian equilibrium potential.¹¹⁻¹⁵ UPD results from the difference in energetics of inter- vs. intralelemental bonding. Therefore, UPD is the formation of a surface compound with the associated heat of formation. In EC-ALE, compounds are grown using a cycle in which an atomic layer of each element is formed in turn, with UPD as the surface-limited process.

Te UPD on Au from acidic electrolytes has been studied previously using EC-scanning tunneling microscopy (STM).^{8,9,16,17} Several structures have been observed on Au(111), including a $1/3$ coverage $(\sqrt{3} \times \sqrt{3})R30^\circ$ -Te with (13×13) light domain walls, a $4/11$ coverage $(\sqrt{7} \times \sqrt{13})$, and a $4/9$ coverage (3×3) -Te. The formation of the (3×3) -Te adlayer coincided with a surface roughening transition. This roughening transition, as well as one preceding the formation of a $5/9$ coverage (3×3) -Te, was observed in the present study as well.

The cyclic voltammetry (CV) obtained for Cd deposition from the solutions used in these studies has been described previously.¹⁸ The insoluble species $\text{Cd}(\text{OH})_2$ forms in basic solutions, so 1 mM H_2SO_4 was chosen as a supporting electrolyte for the Cd deposition solutions. However, Te is soluble in basic or acidic media (though it has been found to be essentially insoluble at neutral pH). Additionally, there is significant pH dependence for Te voltammetry. The deposition features for Te shift to more negative potentials as the pH

increases (Fig. 1). This fact has led to adoption of basic Te solutions for Te deposition steps, as the potentials that may be used then coincide with those used for the Cd deposition steps, and Te can be deposited without oxidizing the Cd UPD layer. Therefore, impetus for the current study is to understand Te deposition from basic Te precursor solutions.

Experimental

For CV and EC-STM, a 99.999% pure Au(111) single crystal (MaTecK GmbH) was used. The Au substrate was cleaned in hot HNO_3 for 30 min, annealed in a hydrogen flame for 7 min, and allowed to cool slowly in air.

The Te and Cd deposition solutions used were composed of 0.25 mM TeO_2 + 10 mM $\text{Na}_2\text{B}_4\text{O}_7$ + 20 mM Na_2SO_4 (pH 9.2), and 0.20 mM CdSO_4 + 1.0 mM H_2SO_4 , respectively. All solutions were prepared with ultrapure water (>18.1 M Ω) and analytical grade reagents. For CdTe deposition studies, Te was deposited on the substrate *ex situ* in a Pyrex H-cell and then the transferred to the EC-STM cell for Cd electrodeposition. EC-STM studies were carried out in constant current mode (height mode) using a Nanoscope III (Digital Instruments, Santa Barbara, CA). The instrument was previously calibrated by imaging highly ordered pyrolytic graphite (HOPG) in air. For all imaging, tips were formed from polycrystalline tungsten wire (diam 0.25 mm) which was etched at 12 V_{ac} in fresh 1 M KOH. To reduce faradaic currents at the tip/electrolyte interface, tips were coated with hot glue-gun glue (Kmart), leaving only the apex exposed. The EC-STM cell has been described previously.¹⁹ The entire setup was isolated from ambient by fitting a Plexiglas hat on top of the microscope and maintaining a positive pressure of high-purity Ar on the system. All potentials were referenced to a 3 M Ag/AgCl reference electrode (BAS), and Au wires served as auxiliary electrodes.

Results and Discussion

pH effect on Te cyclic voltammetry.—A series of thin-layer EC studies were performed to determine the optimal pH for the Te deposition solution (Fig. 1). Scanning negatively in the acidic solutions, the first cathodic peak corresponds to the UPD formation of a $(\sqrt{3} \times \sqrt{3})$ -Te with (13×13) light domain walls. The second peak indicates the formation on the higher coverage (3×3) -Te structure. These features are followed by solvent decomposition (H_2 formation) at more negative potentials. In basic Te deposition solutions, the first peak is related to desorption of the tellurite species as well as the deposition of some Te (see discussion of Te deposition on the Au(100) surface). The $(\sqrt{3} \times \sqrt{3})$ -Te with (13×13) light domain walls formed when the potential was held for several minutes. For pH 10.2 solutions, the second and third peaks represented the for-

* Electrochemical Society Active Member.

^z E-mail: stickney@sunchem.chem.uga.edu

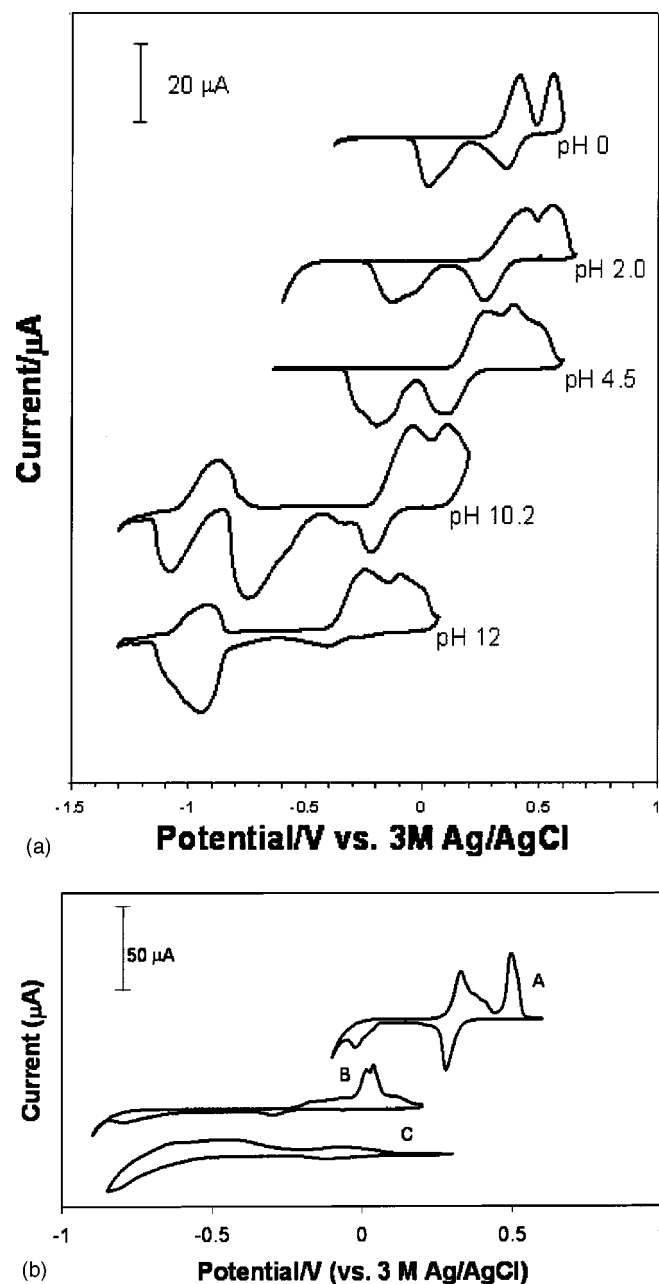


Figure 1. (a) Thin-layer EC study of the effect of pH on Te deposition on a polycrystalline Au electrode. (b) Illustration of how the pH effect on Te CV may be used to facilitate the reductive electrodeposition of Cd and Te in one EC-ALE cycle: (A) Te in pH 2.0 solution, (B) Te in pH 10.2 solution, and (C) Cd in pH 5.7 solution.

mation of the (3×3) -Te structure and formation of the soluble species Te^{2-} , respectively. These two peaks are convolved at pH 12. The voltammetry for the acidic solutions did not exhibit peaks for Te reduction to Te^{2-} , as the potential for Te^{2-} formation exhibited little pH dependence and occurred near -1.1 V in all solutions. However, this potential was not reached in acidic solutions, as solvent decomposition (H_2 formation) occurs prior to Te^{2-} formation. Upon reversing the scan direction, the initial anodic peak is the result of the deposition of Te^{2-} which remained at the electrode surface. The next oxidation features result from the cathodic stripping of the Te layers formed.

When the apex of the initial UPD peak was plotted vs. the solution pH (Fig. 2), the peaks for Te UPD and stripping were revealed

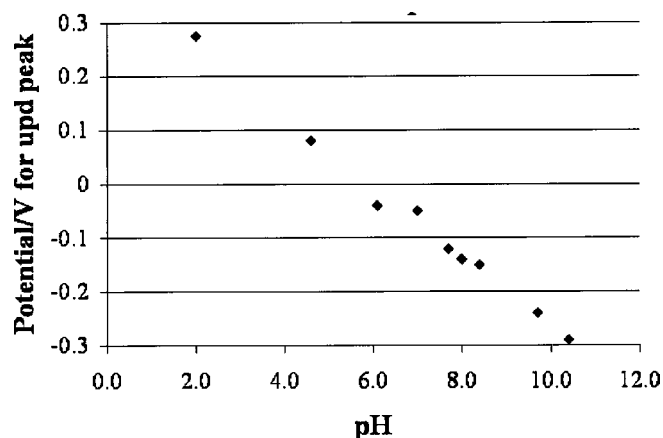


Figure 2. Shift in UPD peak for Te as a function of pH of the deposition solution.

to shift in a linear fashion to more negative potentials as the solution became more basic. The results of this pH study indicated that a basic Te deposition solution would be the most tractable due to the alignment of potentials for Te and Cd UPD (Fig. 1b).

Te atomic layer formation on Au(100).—Previous ultrahigh-vacuum electrochemical (UHV-EC) experiments have suggested that a tellurite species adsorbs on Au surfaces at potentials positive of Te UPD.²⁰ In this study, an ordered (6×6) tellurite species was observed on the Au(100) surface (Fig. 3). This adlayer was observed to exist beside Au islands formed during lifting of the Au(100)- $[(5 \times 20)-(1 \times 1)]$ reconstruction.²¹⁻²³ This reconstruction was produced during annealing and then lifted upon exposure to the tellurite solution. Lifting of the reconstruction resulted in formation of small islands.²⁴ The (6×6) tellurite adlayer was stable on the surface down to -0.13 V, when it apparently desorbed.

As the potential was shifted negatively, a $1/4$ coverage (2×2) -Te adlayer began to form. As the potential was held at -0.3

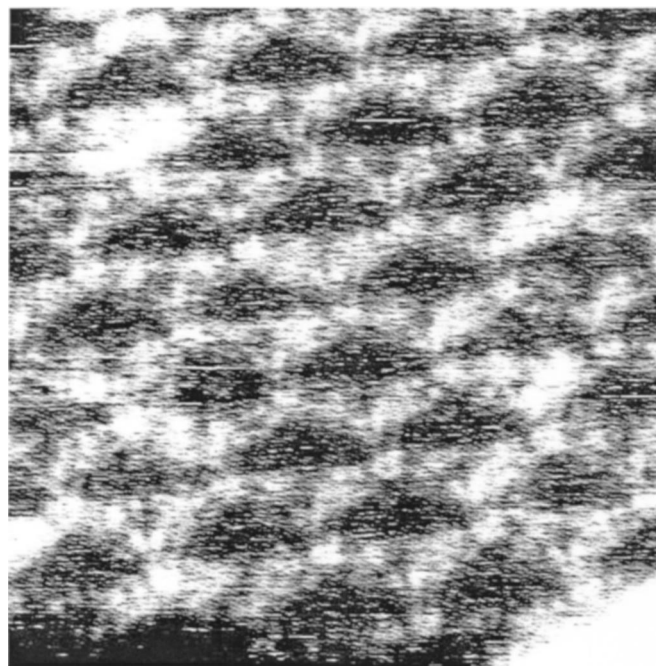
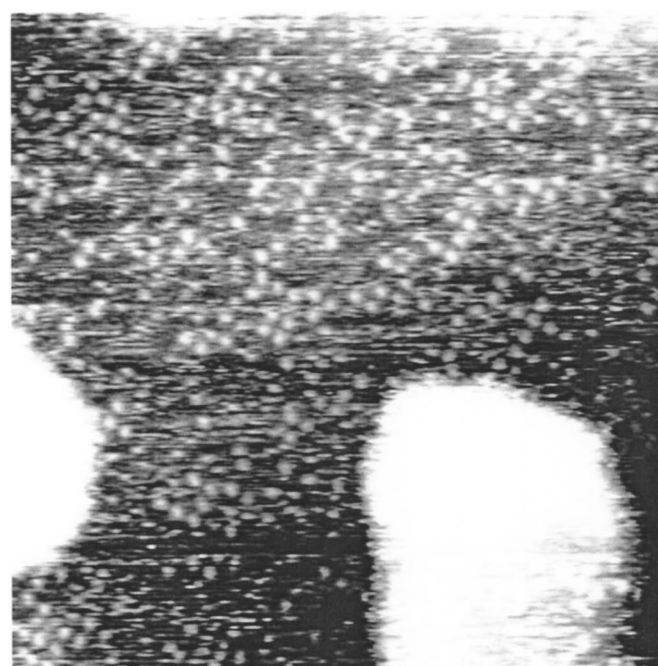
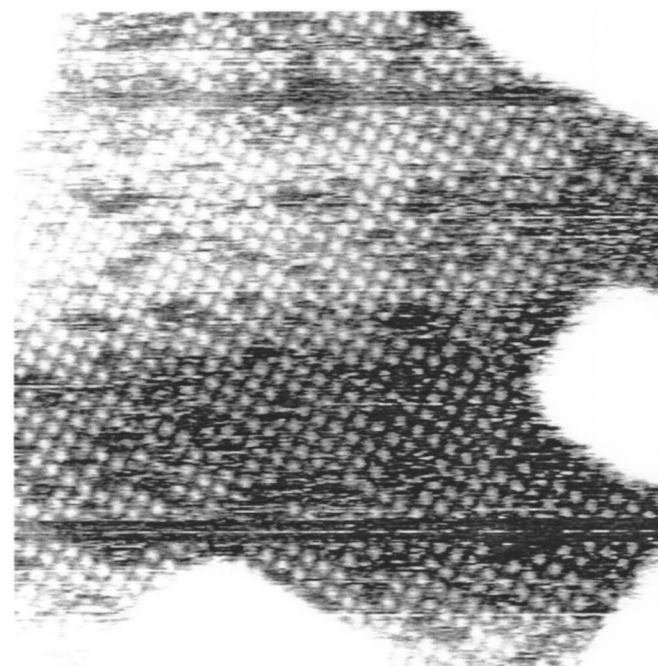


Figure 3. Tellurite adsorbed on a Au(100) surface at open circuit, 0.05 V vs. 3 M Ag/AgCl. Image size 10×10 nm.



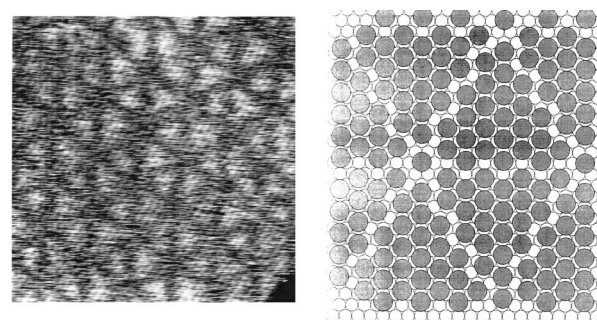
(a)



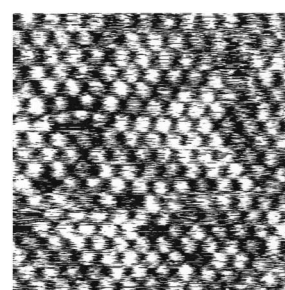
(b)

Figure 4. (a) EC-STM micrograph showing Te atoms adsorbing in random fourfold sites on a Au(100) surface at -0.30 V vs. 3 M Ag/AgCl. Image size is 10×10 nm. (b) After 120 s at -0.30 V vs. 3 M Ag/AgCl, the coverage of adsorbed Te atoms increased, encompassing most of the surface. Image size is 20×20 nm.

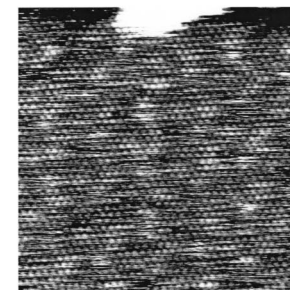
V for 120 s, a transition from the random distribution of Te atoms (Fig. 4a) to a homogeneous (2×2) -Te adlayer slowly took place (Fig. 4b). Again, the Te atoms composing this adlayer were observed to be highly mobile, with the empty four-fold defect sites moving from scan to scan. However, the closest interatomic spacing for the adsorbate was consistently $2a$ (or 2), where “ a ” is the interatomic spacing for Au, 0.288 nm. By scanning the potential to -0.4 V, a $1/3$



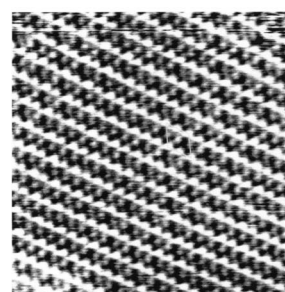
(a)



(b)



(c)



(d)

Figure 5. (a) Image and model of the $1/3$ rd coverage $(\sqrt{3} \times \sqrt{3})$ -Te with (13×13) light domain walls observed at -0.25 V vs. 3 M Ag/AgCl. Image size is 20×20 nm. (b) 8×8 nm EC-STM image of the $(\sqrt{3} \times \sqrt{3})$ -Te with (13×13) light domain walls at -0.3 V vs. 3 M Ag/AgCl. Various single-atom defects are evident. (c) The transition between the $(\sqrt{3} \times \sqrt{3})$ -Te with (13×13) light domain walls and the (3×3) -Te structure. Image size is 20×20 nm. (d) EC-STM micrograph of a $4/9$ coverage (3×3) -Te structure observed at -0.55 V vs. 3 M Ag/AgCl. Image size is 12×12 nm.

coverage $(2 \times \sqrt{10})$ -Te structure, which has been previously observed to form in acidic TeO_2 solutions, appeared.²⁴

Te atomic layer formation on Au(111).—EC-STM experiments showed that if the potential was polarized at -0.20 V on a Au(111) surface, a $(\sqrt{3} \times \sqrt{3})R30^\circ$ -Te with (13×13) light domain walls formed (Fig. 5a). This adsorbate exhibited slow kinetics in the exchange of Te atoms with those in solution, as various single-atom defects were observed at -0.3 V (Fig. 5b). A $(\sqrt{3} \times \sqrt{3})R30^\circ$ -Te with (13×13) light domain walls was observed in UHV-EC experiments after scanning to -0.50 V but was seen at -0.2 V via EC-STM, given sufficient time, because the deposition kinetics are very slow. In fact, *in situ* long-term polarization experiments showed that the higher coverage (3×3) -Te structure is formed at -0.55 V (Fig. 5d). A brief transition period (Fig. 5c), during which an increase in disorder in the adlayer composing the $(\sqrt{3} \times \sqrt{3})R30^\circ$ -Te was observed, was followed by a surface roughening transition and formation of the (3×3) -Te structure (Fig. 5d).

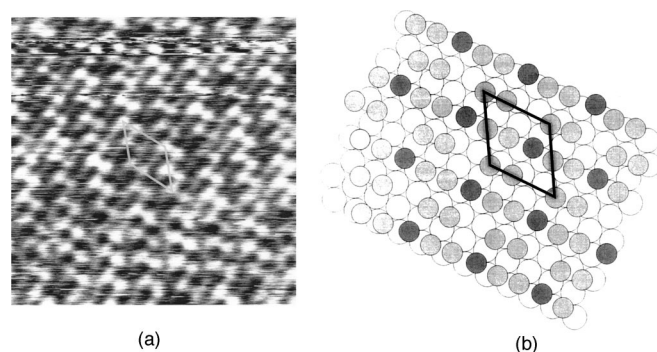


Figure 6. EC-STM micrograph and model of a 6/9 coverage (3×3)-Te structure observed after a roughening transition at -0.70 V vs. 3 M Ag/AgCl. Image size is 5×5 nm.

This roughening transition was evidently a result of stress due to a change in the bond environment of the Te atoms as new bonds to other Te atoms formed when the coverage increased. This resulted in the formation of a series of atomically high plateaus and the 4/9th coverage (3×3)-Te structure. This behavior was also observed in acidic Te solutions at 0.1 V.²⁴

Surface roughening during the formation of higher coverage chalcogenide adlayers can be explained by consideration of the change in bonding that occurs as the coverage is increased. Most chalcogenides form an initial low-coverage structure like the $1/3$ coverage ($\sqrt{3} \times \sqrt{3}$)-Te.²⁵⁻³¹ In this structure, the interatomic spacing, 0.5 nm, is larger than the van der Waals diameter for Te, 0.44 nm.³¹ When the coverage of the chalcogenide is increased until the interchalcogenide distance is less than the van der Waals diameter, the chalcogenide atoms tend to bond together, forming rings, chains, or clusters. This process results in surface stress, because the chalcogenides are bound to each other as well as the Au surface, and this stress results in pits or the roughening transition described previously. The formation of pits and plateaus has been observed previously for Se, S, and alkanethiol adsorption on Au(111) surfaces.^{26,28,32-34}

Stepping the potential to -0.7 V, the surface became disordered, as this potential corresponds to the beginning of bulk Te deposition. To prevent further Te deposition, the potential was then backed off to -0.5 V, positive enough to stop further deposition but negative enough to prevent Te dissolution (Fig. 1). At this potential, a new (3×3)-Te structure, this time at 5/9 coverage, was observed (Fig. 6). This structure was the last observed ordered Te adlayer on Au(111) before bulk deposition.

CdTe formation.—The ($\sqrt{3} \times \sqrt{3}$)-Te with (13×13) light domain walls is fairly stable and can be formed in an H-cell on the bench top, and then transferred to the EC-STM cell for imaging in an acidic Cd solution. When the Te-coated electrode was held at 0.15 V in the acidic Cd solution, the ($\sqrt{3} \times \sqrt{3}$)-Te with (13×13) light domain walls was visible (Fig. 7). Apparently, no Cd had yet deposited, leaving the unperturbed Te structure, and proving the stability of the ($\sqrt{3} \times \sqrt{3}$)-Te with (13×13) light domain walls structure during a transfer through air and immersion in an acidic CdSO₄ solution.

When the potential was shifted to -0.5 V, a severe roughening of the surface occurred. This appears to result from the formation of CdTe. Two issues are suggested to account for this roughening. The first is that it is preferable to form a monolayer of the compound over the entire surface. However, in this case, too little Te was present and a stoichiometric amount of CdTe formed. The rest of the surface was covered by Cd UPD and Au-Cd alloy,^{18,34} giving the impression of a disordered surface.

Another reason for roughening to occur when Cd is deposited on the Te-coated surface is that suddenly there is a monolayer of a



Figure 7. Low-resolution EC-STM micrograph showing the (13×13) light domain walls of an *ex situ* deposited Te layer immersed in a CdSO₄ solution at 0.15 V vs. 3 M Ag/AgCl. Image size is 200×200 nm.

compound bound to the Au surface. This can create strain in the surface if the deposit is not perfectly lattice matched with the substrate. A perfect lattice match is never the case for a heterogeneous deposit, so there may be a periodic array of defects, or even reconstructions of the underlying Au surface, both of which would contribute to an observation of surface roughening.

Aside from the roughening observed on a majority of the surface when Cd was deposited, near step-edges, domains of the ($\sqrt{7} \times \sqrt{7}$)-CdTe structure evident in Fig. 8, were observed. This structure has been previously observed, both with EC-STM and in UHV-EC studies with low-energy electron diffraction.³⁵ There appeared to be two maxima per unit cell, though filtering the image found suggestions of a $3/7$ coverage ($\sqrt{7} \times \sqrt{7}$)-CdTe.

Conclusion

Atomic layers of Te have been grown on Au(100) and Au(111) surfaces from basic tellurite solutions. Although tellurite solutions were observed to lift the Au(111) reconstruction, this could not be attributed to an ordered tellurite species. In contrast, on the Au(100) surface an adsorbed tellurite species with an open (6×6) unit cell was observed at open circuit. Also, in contrast to behavior observed on Au(111) surfaces, Te was observed to deposit in random sites on Au(100), instead of following a nucleation and growth model.

On Au(111), Te nucleated and grew into a $1/3$ ($\sqrt{3} \times \sqrt{3}$) $R30^\circ$ -Te structure with (13×13) light domain walls. Subsequent deposition of Te at more negative potentials resulted in the formation of a 4/9 coverage (3×3)-Te structure and a roughening transition, where the surface was composed of a series of monoatomic islands and pits. The reason for this roughening appears to be strain introduced by the bonding of the chalcogenide atoms to each other, as well as to the Au substrate. At even more negative potentials, the (3×3)-Te at 4/9 coverage was converted into a 5/9 coverage (3×3)-Te. The phase transition from one (3×3) to the next higher coverage (3×3) proceeded through a disordered phase.

CdTe was grown on Au(111) surfaces using a two-step EC-ALE process, consisting of *ex situ* Te UPD from a basic Te solution, followed by *in situ* Cd UPD from an acidic solution. A stoichiometric

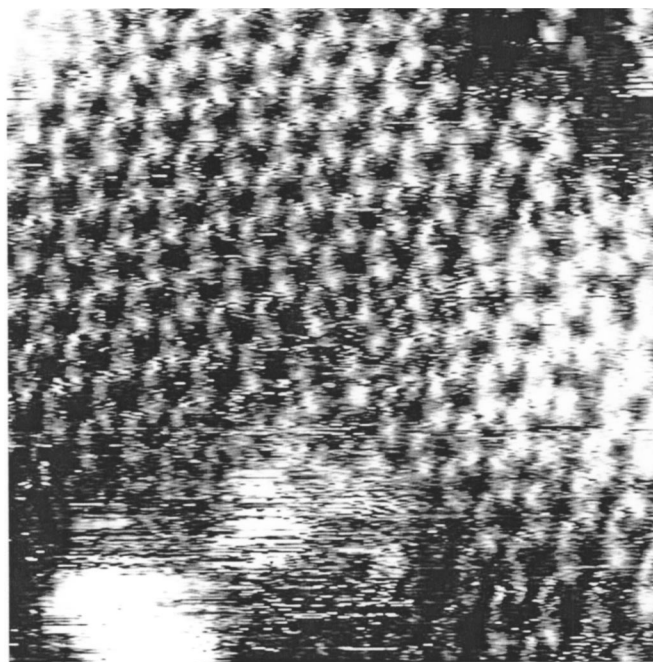


Figure 8. $(\sqrt{7} \times \sqrt{7})$ -CdTe structure observed at -0.50 V vs. 3 M Ag/AgCl. Image size is 10×10 nm.

metric $(\sqrt{7} \times \sqrt{7})R19.1^\circ$ -CdTe structure was observed for Cd deposition on the $1/3$ coverage $(\sqrt{3} \times \sqrt{3})$ -Te structure with (13×13) light domain walls.

The University of Georgia assisted in meeting the publication costs of this article.

References

1. T. Abe, Y. Miki, and K. Itaya, *Bull. Chem. Soc. Jpn.*, **67**, 2075 (1994).
2. R. R. Adzic, N. A. Anastasijevic, and Z. M. Dimitrijevic, *J. Electrochem. Soc.*, **131**, 2730 (1984).
3. R. J. Behm, G. Ertl, and J. Winterlin, *Ber. Bunsenges. Phys. Chem.*, **90**, 294 (1986).
4. K. Abe, H. Takiguchi, and K. Tamada, *Langmuir*, **16**, 2394 (2000).
5. A. J. Bard, H. D. Abruna, C. E. Chidsey, L. R. Faulkner, S. W. Feldberg, K. Itaya, M. Majda, O. Melroy, R. W. Murray, M. D. Porter, M. P. Soriaga, and H. S. White, *J. Phys. Chem.*, **97**, 7147 (1993).
6. D. M. Kolb and H. Gerischer, *Electrochim. Acta*, **18**, 987 (1973).
7. G. F. Fulop and R. M. Taylor, *Annu. Rev. Mater. Sci.*, **15**, 197 (1985).
8. I. Youm, M. Cadene, M. Candille, D. Laplaze, and D. Lincot, *Phys. Status Solidi A*, **140**, 471 (1993).
9. D. L. Batzner, M. E. Oszan, D. Bonnet, and K. Bucher, *Thin Solid Films*, **361**, 288 (2000).
10. D. M. Kolb, in *Advances in Electrochemistry and Electrochemical Engineering*, H. Gerischer and C. W. Tobias, Editors, Vol. 11, p. 125, John Wiley, New York (1978).
11. K. Juttner and W. J. Lorenz, *Z. Phys. Chem., Neue Folge*, **122**, 163 (1980).
12. R. R. Adzic, in *Advances in Electrochemistry and Electrochemical Engineering*, H. Gerischer and C. W. Tobias, Editors, Vol. 13, p. 159, Wiley-Interscience, New York (1984).
13. A. A. Gewirth and B. K. Niece, *Chem. Rev. (Washington, D.C.)*, **97**, 1129 (1997).
14. E. Herrero, L. J. Buller, and H. D. Abruna, *Chem. Rev. (Washington, D.C.)*, **101**, 1897 (2001).
15. B. E. Hayden and I. S. Nandhakumar, *J. Phys. Chem. B*, **101**, 7751 (1997).
16. T. A. Sorenson, D. W. Suggs, I. Nandhakumar, and J. L. Stickney, *J. Electroanal. Chem.*, **467**, 270 (1999).
17. M. D. Lay, K. Varazo, N. Srisook, and J. L. Stickney, *J. Electroanal. Chem.*, **554**, 221 (2003).
18. D. W. Suggs and A. J. Bard, *J. Am. Chem. Soc.*, **116**, 10725 (1994).
19. I. Nacic, C. Shannon, M. J. Bozack, M. Braun, S. Link, and M. El-Sayed, in *Morphological Evolution in Electrodeposition and Electrochemical Processing in ULSI, Fabrication*, P. C. Andricacos, P. Allongue, F. Argoul, D. P. Barkey, J. C. Bradley, K. Kondo, G. M. Oleszak, C. Reidsma-Simpson, P. C. Searson, and J. L. Stickney, Editors, PV 2001-8, The Electrochemical Society Proceedings Series, Pennington, NJ, In preparation.
20. D. M. Kolb, G. Lehmpfuhl, and M. S. Zei, *J. Electroanal. Chem. Interfacial Electrochem.*, **179**, 289 (1984).
21. J. Schneider and D. M. Kolb, *Surf. Sci.*, **193**, 579 (1988).
22. X. P. Gao, A. Hamelin, and M. J. Weaver, *Phys. Rev. Lett.*, **67**, 618 (1991).
23. Y. J. He and E. Borguet, *J. Phys. Chem. B*, **105**, 3981 (2001).
24. T. A. Sorenson, K. Varazo, D. W. Suggs, and J. L. Stickney, *Surf. Sci.*, **470**, 197 (2001).
25. M. D. Lay, K. Varazo, and J. L. Stickney, *Langmuir*, **19**, 8416 (2003).
26. X. P. Gao, Y. Zhang, and M. J. Weaver, *J. Phys. Chem.*, **96**, 4156 (1992).
27. T. E. Lister and J. L. Stickney, *J. Phys. Chem.*, **100**, 19568 (1996).
28. G. Andreasen, C. Vericat, M. E. Vela, and R. C. Salvarezza, *J. Chem. Phys.*, **111**, 9457 (1999).
29. C. Vericat, G. Andreasen, M. E. Vela, and R. C. Salvarezza, *J. Phys. Chem. B*, **104**, 302 (2000).
30. H. Martin, C. Vericat, G. Andreasen, A. H. Creus, M. E. Vela, and R. C. Salvarezza, *Langmuir*, **17**, 2334 (2001).
31. L. Pauling, *The Nature of the Chemical Bond*, 3rd ed., Cornell University Press, Ithaca, NY (1960).
32. R. L. McCarley, Y. T. Kim, and A. J. Bard, *J. Phys. Chem.*, **97**, 211 (1993).
33. I. Touzov and C. B. Gorman, *J. Phys. Chem. B*, **101**, 5263 (1997).
34. M. D. Lay and J. L. Stickney, *J. Am. Chem. Soc.*, **125**, 1352 (2003).
35. K. Varazo, M. D. Lay, T. A. Sorenson, and J. L. Stickney, *J. Electroanal. Chem.*, **522**, 104 (2002).